Models for Simulation Based Selection of 3D Multilayered Graphene Biosensors

E. Lacatus *[1], G.C. Alecu[1], and A. Tudor[1]
[1]Polytechnic University of Bucharest
* E. Lacatus: elena.lacatus@upb.ro

Abstract: At the forefront of a new generation of sensors grapheme and grapheme composite materials are intensively studied for medical and biosensing applications. The outstanding electrical, mechanical and quantum properties of grapheme make them a promising material solution to overlap the existing gap between biological and non-biological systems into a continuum like-viscoelastic integrated model.
Through COMSOL Multiphysics ® modeling and simulation were identified the best fitted solutions for a multilayered biosensing device structure from the presently known graphene (G), graphene- oxide (GO) and composite materials including different forms of graphene (graphene nanoribbons –GNRs, reactive graphene oxide –RGO, and TWEEN paper –TwGP).

Keywords: graphene, biosensor, Fröhlich quantum coherence, phonon, non-linear thermodynamics

1. Introduction

Intensely studied in the last decade, graphene (G), graphene oxides (GO), reactive graphene oxides (RGO), graphene nanoribbons (GNRs) and many other graphene based composite materials are continuously approach to the medical and biosensing area with the aim of defining new material solutions for properly personalized medical applications and therapeutic solutions.

With large similarities to the surface of graphite (Figure 1), graphene (G) can adsorb and desorb different type of atoms and molecules, remaining highly conductive [1]. This property can be used for sensor applications. It is largely known that single- layer graphene (1G) is much more reactive than 2G, 3G (<10 layers) graphene multilayer structures [2,3]. However, the edge of the graphene is more reactive than the surface, graphene being a fairly inert material, and thus an ideal candidate for bio-sensors.

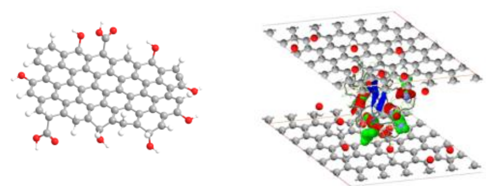

a b

Figure 1. (a) Graphene model; (b) Functionalized bilayer-graphene structure *(ChemBio 3D Ultra©)*

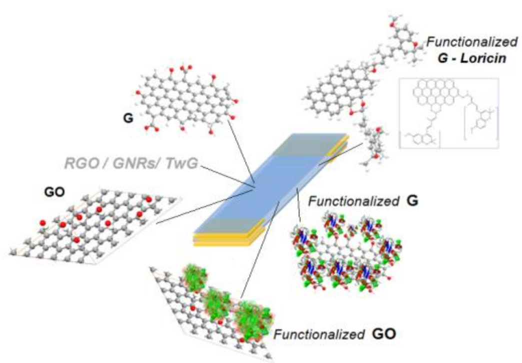

Figure 2. Basic and functionalized graphene structures *(ChemBio 3D Ultra©)*

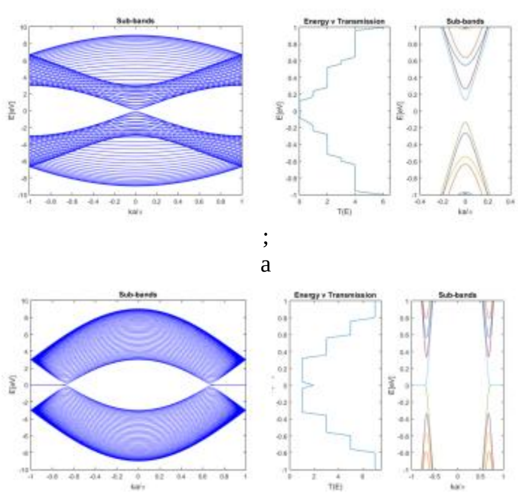

;
a

b

Figure 3. MATLAB© models of electronic properties of graphene :(a) 20 atoms – armchair structure;
(b) 20 atoms – zig-zag structure

The aim of the modeling and simulation of the multilayered graphene structures is mainly focused on the device response at different types of energy stimulus reaching the active surfaces of the 3D bio-sensing structures under the main restrictions of biocompatibility and non-toxicity (Figure 2, Figure 3).

2. Models Definition

The most accessible and nonintrusive interface of a sensor with humans is on the skin surface. Not only because skin is the organ that has the widest area of the human body, but because it has differentiated responses to internal and external stimuli, thus being an accessible environment for physical and chemical data gathering.Based on FET (Field Effect Transistor) properties [15,17] that can relate human skin to the presently known characteristics of G/GO/TwGP [1,4,5,13,16,18] two biosensing devices were designed (Figure 4 c, d).

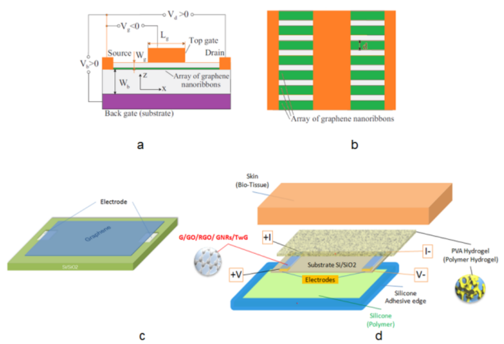

Figure 4 Multilayer graphene sensing concepts: (a),(b) General GNRs multilayer concept [4,18] (c) single layer G/GO sensor; (d) multilayer G/GO/TwGP sensor

For these studies were considered the main interfaces between: human skin – hydrogel polymer structure (PVA Hydrogel); PVA Hydrogel – graphene based module (G/GO/TwGP); graphene module – electrodes (Ag); graphene/electrodes – substrate (Silica glass SiO_2) (Figure 4 c, d).For each of these interfaces were identified models able to describe the evolution of the process microvariables as well as the environmental stimuli influences (macrovariables) as follows:

- Two electrodes biosensing module (Figure 4c) including skin, PVA Hydrogel, graphene (G) and graphene-oxide (GO) functionalized with different proteins (Alpha Helix, Loricin and Lysozyme)
- Four electrodes module (Figure 4 d) that considers the same main interfaces with both graphene composite structure and without it, for the same environmental stimuli, in order to objectively differentiate the graphene responses (Figure 5,…15)

All these models are having the same continuum-like background of a biosensor device structure based on weak van der Waals interaction forces that describe the nonlinear behavior of graphene into a surrounding viscoelastic environment through classical Kirchhoff plate theory [14]

In the Equation 1, used for modeling single layer graphene vibration response based on Kirchhoff plate theory [14] α_1 and α_3 represents the linear and nonlinear interaction forces:

$$D\nabla^4 w + \alpha_1 w + \alpha_3 w^3 + \rho h \frac{\partial^2 w}{\partial t^2} + N_x \frac{\partial^2 w}{\partial x^2} + N_y \frac{\partial^2 w}{\partial y^2} = 0 \qquad (1)$$

where: *Nx*, *Ny* are biaxial in-plane loads; *a*, *b*- length, width of the single layer graphene; *h*-thickness of the single layer graphene; *p* – distributed transverse load per unit area (due to surrounding medium effect) ; *D* is the bending stiffness of the plate:

$$D = \frac{Eh^3}{12(1-\nu^2)} \qquad (2)$$

E is the Young's modulus; *ν* – Poisson's ratio; *ρ* – mass density; ∇^2 - Laplace operator:

$$\nabla^2 = \frac{\partial^2}{\partial x^2} + \frac{\partial^2}{\partial y^2} \qquad (3)$$

The density of charge, characterizing all interfaces, is properly described through nonlinear thermodynamics with electron – phonon *(ē – ph)* , phonon – phonon *(ph – ph)* and *ion –phonon* interactions. Thus for all models were studied the charge density distributions of electric, thermal and acoustic field stimuli responsible for *(ē – ph), (ph – ph)* and *(ion –ph)* interactions (Figures 5,…, 15).

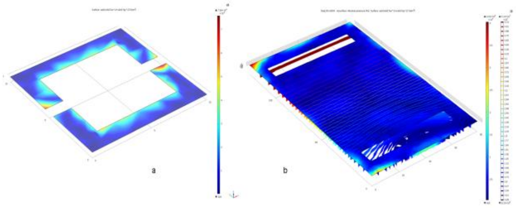

Figure 5. Substrate (SiO_2) stress distribution
(a) 2 electrodes device; (b) 4 electrodes device

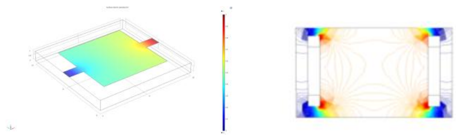

a b

Figure 6. Electric potential on interface:
(a) 2 electrodes device; (b) 4 electrodes device

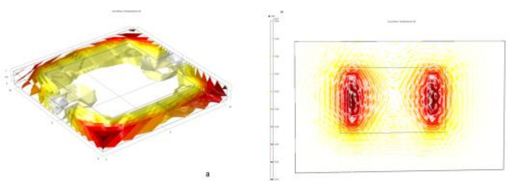

Figure 7. Temperature distribution at interface (isosurfaces) (a) 2 electrodes device; (b) 4 electrodes device

3. Use of COMSOL Multiphysics

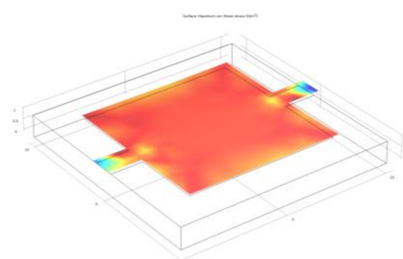

a

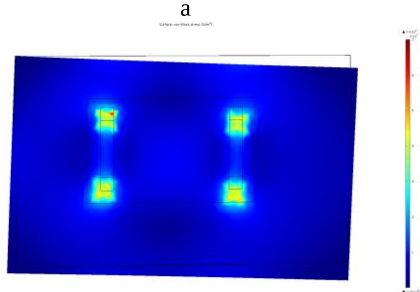

b

Figure 8. von Misses stress shell:
(a) 2 electrodes device; (b) 4 electrodes device

For the envisaged multilayer structures of graphene biosensing devices a graphene model was firstly created in ChemBio 3D Ultra©. Its characteristics have been exported to MATLAB© and thus different process parameters and material properties were consistently interlinked for further analyses and simulations (Figure 2,3).

MATLAB© model and the associated properties were exported through the LiveLink™ for MATLAB© add-on in COMSOL Multiphysics ® and thus the variability of the structure properties (Figure 3) could be properly analyzed in at the device scale (Figure 5,…,15).
The models designed to include environmental stimuli acting upon human body were focused either on the thermal slight modifications or electric conductance variations due to emotional rose or on area exposure to acoustic waves (Figure 6,7). Acoustic Module of COMSOL Multiphysics ® and Equation Based Models were used to define interface response to variations of environment acoustic pressure (frequency vary from 1000 Hz to 8000 Hz)

4. Results

A large number of device module types have been tested in order to define the best response of the hydrogel- polymer layer (PVA Hydrogel) on the graphene sheets and of the protein functionalized graphene biosensors.

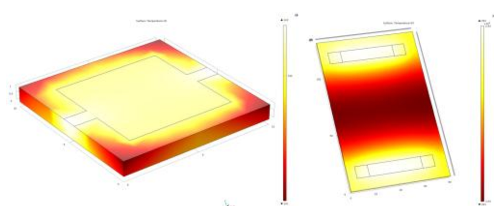

Figure 9. Temperature distribution :
(a) 2 electrodes device; (b) 4 electrodes device

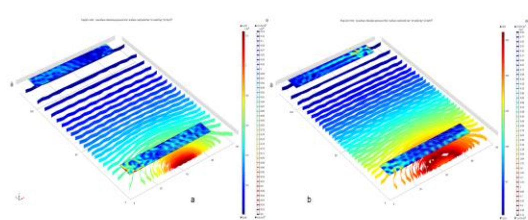

Figure 10Acoustic stimuli over graphene sensing structure(4 electrodes device): (a) *f*=1500Hz;
(b) *f*=7000 Hz

For each of these modules the biologic responses and the field excitations have to reach simultaneity under the COMSOL Multiphysics ® model (Figure 4).

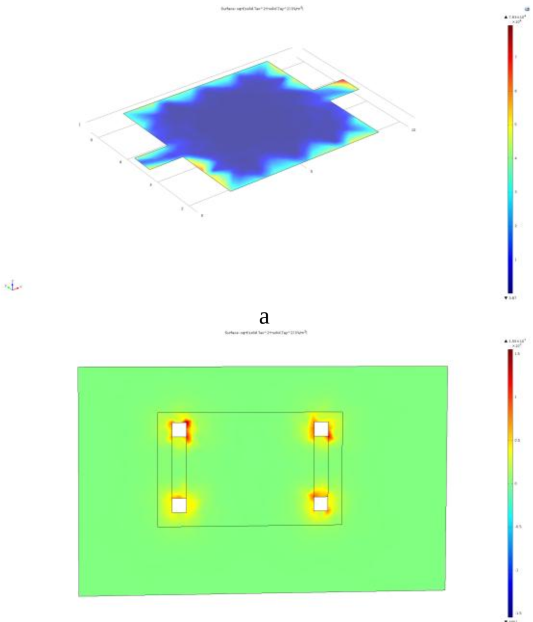

Figure 11 Pressure distribution (skin-polymer)/sensor interface: (a) 2 electrodes device; (b) 4 electrodes device

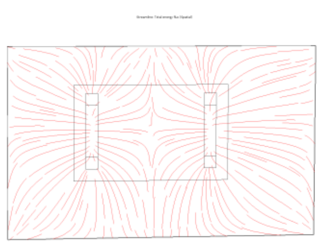

Figure 12 Spatial distribution of flux energy on graphene bisensor (4 electrodes device)

.

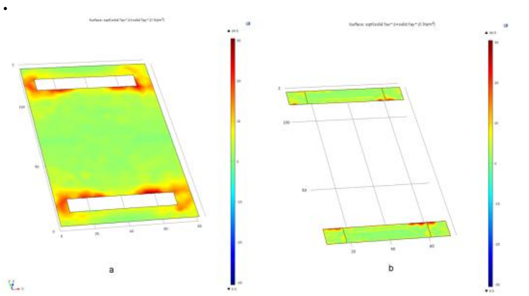

Figure 13 Interfaces charge distributions (4 electrodes device)

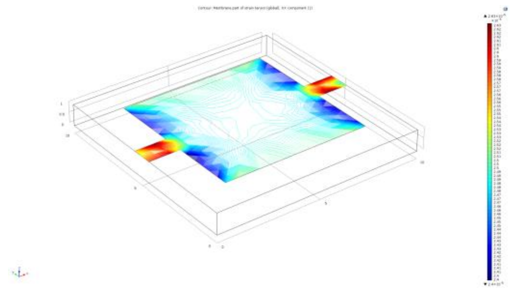

Figure 14 Membrane stress under environmental stimuli: 2 electrodes device

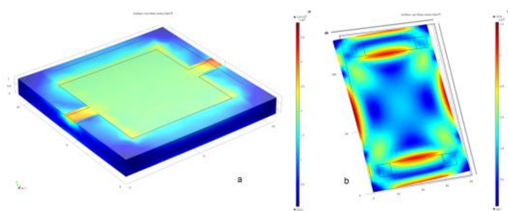

Figure 15 Interface stress under environmental stimuli: (a) 2 electrodes device; (b) 4 electrodes device

5. Discussion

The analyzed biosensing device models, regardless their design solution (two or four electrodes; single- or multilayer graphene; graphene composite material) revealed through simulations output data the “sensing” ability of the graphene –based concept model.

For each module type the graphene/ graphene composite materials generate clearly differentiate responses to the environmental stimuli, or process microvariables evolution, thus confirming the biosensing ability of this class of materials.

Operating with a continuum model for all interfaces *($\bar{e}$ – ph, ph – ph* and *ion –ph)* and harvesting biological charge density variations to relate them to environment stimuli, the 3D multilayered graphene biosensors models and simulations offered valuable design solutions

6. Conclusions

Making the best use of the flexible modules of COMSOL Multiphysics ® the most relevant device properties of the multilayered graphene biocompatible structures could be determined and, mostly important, could be related to the complex interface phenomena at human skin level.

7. References

1. J.-C Charlier, et al., *Electron and Phonon Properties of Graphene: Their Relationshop with Carbon Nanotubes , Carbon Nanotubes,* Springer-Verlag, Berlin, http://dx.doi.org/10.1007/978-3-540-72865-8_21, (2008)
2. H. Fröhlich , F. Kremer, *Coherent Excitations in Biological Systems* , Springer-Verlag, ISBN 978-3-642-69186-7,(1983)
3. H.Fröhlich, *Biological Coherence and Response to External Stimuli* , Springer, ISBN 978-3-642-73309-3, (1988)
4. A.K. Geim, K.S. Novoselov , *The rise of graphene*. Nat. Mater. 6, 183, (2007)
5. O. Heinonen, P.L. Taylor, *A Quantum Approach to Condensed Matter Physics*; Cambridge University Press: Cambridge, UK, 2002.
6. B. Hille, *Ion Channels of Excitable Membranes*, Sinauer, (2001)
7. E. Lacatus, *Engineering Self-Assembly through Modeling Nanostructures*, EngOpt 2010, The 2nd International Conference on Engineering Optimization, 6-9 September 2010, Lisbon, Portugal, ISBN 978-989-96264-3-0, (2010)
8. E. Lacatus, F.A. Savulescu, *Nano-Bio-Cogno Model of Acoustic Patterning for Molecular Neurostimulation*, ASME Proceedings DOI:10.1115/FMD2013-16178, (2013)
9. E. Lacatus, *Ion Channel Path of Cellular Transduction*, Biochimica et Biophysica Acta (BBA), Bioenergetics Volume 1837, p.110-111, DOI: 10.1016/j.bbabio.2014.05.266, (2014)
10. E. Lacatus, et al., *Analysis of 3D Biocompatible Additive Structure Using COMSOL Multiphysics® Software*, COMSOL Conference , Cambridge , (2014)
11. E. Lacatus, et al., *From Music to Non-Invasive Therapies via COMSOL Multiphysics® Models*, COMSOL Conference, Cambridge, (2014)
12. E. Lacatus, *Modeling a Multilayered Graphene Biosensing Structure*, 6th International conference on Advanced Nano Materials, Aveiro, (2015)
13. D.L. Mafra, P.T. Araujo, *Intra- and Interlayer Electron-Phonon Interactions in BiLayer Graphene*, Appl. Sci. 2014, 4, 207-239; doi:10.3390/app4020207, (2014)
14. M.H. Mahdavi et al., *Nonlinear vibration and postbuckling analysis of a single layer graphene sheet embedded in a polymer matrix*, Physica E 44 1708–1715, (2012)
15. M.V. Mesquita et al., *Systems Biology: An Information-Theoretic-Based Thermo-Statistical Approach*, Brazilian Journal of Physics, vol. 34, no. 2A, June, (2004)
16. A.H.C. Neto et al., *The electronic properties of graphene*. Rev. Mod. Phys. 81, 109–162, (2009)
17. P.V. Tsaklis, *Presentation of acoustic waves' propagation and their effects through human body tissues*, Human Movement, 58, vol. 11 (1), 58–65, DOI: 10.2478/v10038- 009-0025-z, (2010)
18. D. Verma et al., *Vibration mode localization in single- and multi-layered graphene Nanoribbons*, Computational Materials Science 95,41–52, (2014)

8. Appendix

MODEL LIBRARY: Device SLGS (G/GO)
E.g.: Material 1 -Silica Glass

Model Parameters	**Details**
Definitions	Input voltage, Layer thickness, Electric conductivity of silver, Electric conductivity of Nichrome, Air temperature Heat transfer film coefficient, Air Fluid temperature, Heat transfer film coefficient, fluid
Material 1	**Silica Glass**
Material 1 Parameters	Coefficient of thermal expansion Heat capacity /constant pressure Density, Thermal conductivity Young's modulus ,Poisson's ratio
Equations Material 1	$0 = \nabla \cdot s + F_V$ $s = S_0 + C : (\epsilon - \epsilon_0 - \epsilon_{inel})$ $\epsilon = \frac{1}{2}\left(\nabla \mathbf{u} + (\nabla \mathbf{u})^T\right)$

Mesh	Normal; Number of degrees of freedom solved for: 2761 (plus 210 internal DOFs).
Solver configuration	COMSOL Multiphysics AC/DC Module CAD Import Module Heat Transfer Module Structural Mechanics Module
Plot groups	Stress (Solid), Isosuface : Total stored energy

For each material and interface layer of both devices were generated similar reports.

MODEL LIBRARY: Acoustic stimulation of devices MLGS (G/GO/TwGP)

Model Parameters	**Details**
Definitions	Input voltage, Layer thickness, Electric conductivity of silver, Electric conductivity of Nichrome, Air temperature Heat transfer film coefficient, Air Fluid temperature, Heat transfer film coefficient, fluid
Used modules	COMSOL Multiphysics AC/DC Module CAD Import Module Heat Transfer Module Structural Mechanics Module
Material 1	**Substrate (Si)**
Material 2	**Silica Glass**
Material 3	**Electrodes**
Material 4	**TWEEN/RGO (TwGP)**
Material 1 Parameters	Coefficient of thermal expansion; Heat capacity /constant pressure Density Thermal conductivity Young's modulus Poisson's ratio
Equations Material 1	$-\nabla \cdot \sigma = \mathbf{F}_V$
Equations Material 2	$0 = \nabla \cdot s + \mathbf{F}_V$ $s = S_0 + C : (\epsilon - \epsilon_0 - \epsilon_{inel})$ $\epsilon = \frac{1}{2}\left(\nabla \mathbf{u} + (\nabla \mathbf{u})^T\right)$
Equations Material 3	$-\nabla \cdot \sigma = \mathbf{F}_V + 6(\mathbf{M}_V \times \mathbf{n})\frac{z}{d^2}$ $\sigma_z = 0, \quad -\frac{d}{2} \leq z \leq \frac{d}{2}$
Equations Material 4	$-\mathbf{n} \cdot (-k\nabla T) = d_s Q_s - \nabla_T \cdot (-d_s k_s \nabla_T T)$
Mesh	Normal; Number of degrees of freedom solved for: 2761 (plus 210 internal DOFs).
Frequency domain	Frequencies: range(1000,500,8000)
Solver configuration	COMSOL Multiphysics AC/DC Module Heat Transfer Module Structural Mechanics Module Acoustic module
Plot groups	Stress (Solid), Temperature (ht); Isothermal Contours (ht), Electric Potential (ecs); Stress (shell); non-deformed Geometry (shell); surface losses (*freq.*1000-8000Hz); Interface stress 01(*freq.*1000-8000Hz); Interface stress 02(*freq.*1000-8000Hz); Displacement (*freq.*1000-8000Hz); Temperature (due vibration); Mesh contour; Acoustic pressure 01; Acoustic pressure 02; Acoustic pressure 03;

For each material and interface layer of the biosensing devices were generated similar reports with and without acoustic stimulation.